Journal of *Marine Science and Engineering*

MDPI

Article

Arsenic Adsorption and Toxicity Reduction of An Exopolysaccharide Produced by *Bacillus licheniformis* B3-15 of Shallow Hydrothermal Vent Origin

Antonio Spanò [1,2,†], Vincenzo Zammuto [1,2,3,†], Angela Macrì [1], Eleonora Agostino [1], Marco Sebastiano Nicolò [1,2], Angela Scala [1], Domenico Trombetta [1], Antonella Smeriglio [1], Mariarosaria Ingegneri [1], Maria Teresa Caccamo [4], Salvatore Magazù [2,3,4], Miguel Martinez [2,5], Carla Geraldine Leon [2,5], Salvatore Pietro Paolo Guglielmino [1,2] and Concetta Gugliandolo [1,2,*]

[1] Department of Chemical, Biological, Pharmaceutical and Environmental Sciences, University of Messina, Viale Ferdinando Stagno D'Alcontres 31, 98166 Messina, Italy
[2] Research Centre for Extreme Environments and Extremophiles, University of Messina, Viale Ferdinando Stagno D'Alcontres 31, 98166 Messina, Italy
[3] ATHENA Green Solutions S.r.l., Viale Ferdinando Stagno D'Alcontres 31, 98166 Messina, Italy
[4] Department of Mathematical and Computer Sciences, Physical and Earth Sciences, University of Messina, Viale Ferdinando Stagno D'Alcontres 31, 98166 Messina, Italy
[5] Department of Microbiology, Faculty of Biological Sciences, Universidad de Concepcion, Concepcion 4070386, Chile
* Correspondence: concetta.gugliandolo@unime.it
† These authors contributed equally to this work.

Abstract: Exopolysaccharide (EPS) production represents an adaptive strategy developed by extremophiles to cope with environmental stresses. The EPS-producing *Bacillus licheniformis* B3-15, of shallow marine vent origin (Vulcano Island, Italy), was previously reported as tolerant to arsenate (As^V). In this study, we evaluated: (i) the increasing production of EPS by *Bacillus licheniformis* B3-15 in the novel SG17 medium; (ii) the arsenic absorption capacity of the EPS by mass spectroscopy; (iii) the functional groups of EPS interacting with As by ATR-FTIR spectroscopy; and (iv) the ability of EPS to prevent arsenic toxicity by the bioluminescent assay. The EPS yield (240 mg L^{-1}) was 45% higher than previously reported. The EPS was mainly constituted of disaccharide repeating units with a manno-pyranosidic configuration and low protein content, attributed to the poly-gamma glutamic acid component as evidenced by NMR analysis. ATR-FTIR spectra indicated that the functional groups of the EPS (O–H, C=O, C–O and C=C and N–O) were involved in the adsorption of the arsenic cations, with greater interactions between EPS and arsenate (As^V) than arsenite (As^{III}). Consequently, the EPS at increasing concentration (100 and 300 µg mL^{-1}) adsorbed As^V more efficiently (20.5% and 34.5%) than As^{III} (0.7% and 1.8%). The bioluminescence assay showed that the EPS was not toxic, and its addition reduced the toxicity of both As forms by more than twofold. The crude EPS B3-15 could be used in arsenic bioremediation as a possible eco-friendly alternative to other physical or chemical methods.

Keywords: *Bacillus*; exopolysaccharides (EPSs); arsenic contamination; shallow-hydrothermal vent; thermophiles; ecotoxicology

Citation: Spanò, A.; Zammuto, V.; Macrì, A.; Agostino, E.; Nicolò, M.S.; Scala, A.; Trombetta, D.; Smeriglio, A.; Ingegneri, M.; Caccamo, M.T.; et al. Arsenic Adsorption and Toxicity Reduction of An Exopolysaccharide Produced by *Bacillus licheniformis* B3-15 of Shallow Hydrothermal Vent Origin. *J. Mar. Sci. Eng.* **2023**, *11*, 325. https://doi.org/10.3390/jmse11020325

Academic Editor: Casotti Raffaella

Received: 31 December 2022
Revised: 26 January 2023
Accepted: 31 January 2023
Published: 2 February 2023

1. Introduction

Arsenic (As) is a metalloid widespread in the environment, originating from either geogenic and anthropogenic sources, whose toxicity depends on its concentration and speciation [1]. Its most toxic and prevailing forms in aqueous systems are arsenite (As^{III}), which is present under anoxic or reduced conditions, and arsenate (As^V), which prevails in soils and oxygenated surface waters [2,3]. High concentrations of natural arsenic in groundwater have severe human health impacts, ranging from skin lesions to cancer of the brain, liver, kidney,

and stomach [3 and the references therein]. Therefore, the presence of arsenic in water often limits its use as drinking water in several parts of the world [4–6]. The European Directive 98/83/EC imposed the limit of arsenic in drinking water to 10 μg L^{-1}. Conventional strategies for water and soil remediation are either expensive or they usually generate toxic by-products with negative impacts on ecosystems. Therefore, there is growing interest in biologically-based approaches to find environmentally safe strategies such as biosorption through microbial biomass and their products [7].

Generally, microorganisms have developed resistance strategies in response to toxic concentrations of heavy metals that include nonspecific and specific mechanisms involved in metabolic and enzymatic reactions [7,8]. Metabolic pathways that confer resistance to bacteria are codified by genes for the arsenate reduction (*ars* system) and the arsenite oxidation (*aio* system). Among the nonspecific mechanisms, the production of bacterial exopolysaccharides (EPSs), as either attached (loosely bound) to the cell surface or excreted by bacteria to forming complex biofilm structures, contributes to constitutive, nonspecific mechanisms involved in the microbial metal resistance or tolerance [5,9,10]. EPSs, showing biosorption activity for metal ions, favor their sequestration and hence obstruct them from penetrating the cell surface [7]. EPSs composition may vary widely, as they may be homo- or hetero-polysaccharides and may contain different organic and inorganic substituents such as sulfate, phosphate, acetic acid, and acetylate [11,12]. EPSs can also possess small proportions of proteins and uronic acids [13,14]. Generally, biosorption occurs by interaction between negatively charged EPSs and positively charged metal ions (i.e., As, Cu, Pb, and Cd), resulting in their immobilization [15,16].

Shallow hydrothermal systems of the Eolian Islands (Italy), characterized by unusual environmental conditions for most organisms (high temperatures, low pH values, and the release of high concentrations of CO_2, H_2S, and hydrocarbons), provide interesting examples of extreme marine environments where fluids also expel high concentrations of heavy metals that are released from the sea–water–rock interaction at elevated temperatures [17–24]. Thermophilic bacilli (with optimal growth at temperatures ranging from 45 to 70 °C) from Eolian vents are ideal candidates for experimentally addressing questions to extend our knowledge of the resistance strategies to cope with environmental stresses [25–27]. A variety of novel thermotolerant and thermophilic bacilli have previously been isolated from these sites, and most of them were tolerant to heavy metals. Several *Bacillus* and *Geobacillus* spp., isolated from vents of Panarea Is., have displayed a tolerance to mercury [28]; *Geobacillus* sp. strain 5-2, isolated from a vent of Lipari Is., was tolerant to zinc [29] and *B. licheniformis* strain B3-15, isolated from a vent of Vulcano Is., was resistant to Cd^{II}, Zn^{II}, As^{V}, and Hg^{II} [30]. Biomolecules (such as enzymes, biosurfactants, and EPSs) from thermophilic Eolian bacilli possess attractive physical, chemical, and rheological properties and biological activities, which make them useful in several biotechnological applications [28–33]. Many of these strains including *B. licheniformis* B3-15 were able to produce thermostable, water soluble, and non-cytotoxic EPSs, with antiviral, immunostimulant, and immunomodulator activity, useful in pharmaceutical applications [34–39].

We supposed that EPSs may play a key role in coping with extreme physicochemical conditions at the Eolian hydrothermal vents, and also protect the in situ cells by binding the heavy metals released from the vents, in order to improve their bioavailability or to decrease their toxicity [28,29].

In an ongoing search for new environmentally friendly biomolecules useful for arsenic biosorption, the aims of this work were: (i) to enhance the EPS production by *B. licheniformis* B3-15 in a novel medium; (ii) investigate the arsenic adsorption capacity of the EPS; and (iii) identify the functional groups of the EPS interacting with arsenic. Moreover, the ability of the EPS to prevent the toxic effects of arsenic was tested by the bioluminescent assay.

2. Materials and Methods

2.1. Bacillus licheniformis Strain B3-15

Bacillus licheniformis strain B3-15, as a producer of the exopolysaccharide EPS B3-15, has previously been described [30]. Briefly, the strain B3-15 was isolated from a thermal fluid sample collected at a 0.7 m depth from a shallow hydrothermal vent located at Porto di Levante (Vulcano, Eolian Islands, Italy). The strain grew aerobically from 25 to 60 °C and its optimal temperature occurred at 45 °C. The pH range for growth was 5.5–9 with the optimum at pH 7 while the strain grew in a range of 0–7% (*w*/*v*) of NaCl and optimally with 2% (*w*/*v*) NaCl. The partial 16S rRNA gene sequence was submitted to GenBank under accession number: KC485000. The EPS was produced in MD162 mineral medium deprived of tryptone and amended with glucose 0.6%, and its yield was 165 mg L^{-1}. After purification, the EPS2 fraction, with carbohydrates (66%), mainly represented by mannose, and proteins (5%), was a tetrasaccharide repeating unit essentially constituted by sugars with a manno-pyranosidic configuration.

To test the susceptibility to arsenic of *B. licheniformis* B3-15, the medium Marine Broth (MB, Condalab, Madrid, Spain) diluted 1:4 ($MB\frac{1}{4}$) was used to minimize the metal complexation. Arsenic was added from filter-sterilized stock solutions of $NaAsO_2$ (As^{III}) or Na_2HAsO_4 $7H_2O$ (As^{V}) in deionized water at different final concentrations (500, 1000, 1500, and 2000 μg mL^{-1}).

An overnight bacterial culture in Tryptone Soy Broth (Condalab, Madrid, Spain) plus 1% of NaCl after incubation at 45 °C was centrifuged at 8000× *g* for 10 min. The bacterial pellets (OD_{600nm} = 0.1) were resuspended in $MB\frac{1}{4}$ and inoculated (2 mL) in each tube (18 mL) containing As^{III} or As^{V}, or without As as the control. The tubes were incubated at 45 °C in a rotary shaker (200 rpm) and the growth was evaluated spectrophotometrically (OD_{600nm}) after 24, 48, and 72 h. Absorbance values (OD_{600nm}) ≤ 0.2 were indicative for "no growth" (−), those ranging from 0.2 to 0.5 for "low growth" (+), from 0.5 to 0.8 for "medium growth" (++), and ≥0.8 for "high growth" (+++).

2.2. EPS B3-15 Production and Characterization

To improve the EPS yield, strain B3-15 (OD_{600nm} = 0.1) was inoculated in the novel mineral medium, named SG17, containing 5% of glucose as a carbon source (Table 1) and flasks were incubated at 45 °C for 48 h under shaking conditions at 250 rpm.

Table 1. SG17 element composition.

	Concentration (g L^{-1})
NaCl	47.19
KCl	0.55
NaBr	0.07
H_3BO_3	0.022
NaF	0.0024
NH_4Cl	1.07
K_2HPO_4	0.8
KH_2PO_4	0.2
$NaHCO_3$	0.16
Yeast extract	1
Meat extract	1
Borate buffer 1 M	10
pH $FeCl_3 \times 6H_2O$	0.001
$MgSO_4$	1
$SrCl_2$	0.01
Glucose	50
pH	7

The culture was centrifuged at 8000× *g* for 10 min, and the cell-free supernatant (CFS) was obtained by filtering through a 0.2-μm-pore-size membrane (Biogenerica, Catania,

Italy). To ensure that no cells were present in the filtrates, 100 µL was spread onto plates of Tryptic Soy Agar (Condalab, Madrid, Spain) and incubated at 45 °C for 24 h. To inactivate the enzymes responsible for the EPS degradation, the CFS was heated at 100 °C for 20 min. The CFS was treated with an equal volume of cold absolute ethanol added dropwise under stirring in an ice bath, held at −20 °C overnight, and then centrifuged at 10,000× *g* for 30 min. The pellet was washed twice with ethanol, dissolved in hot water (80–90 °C), and dialyzed (6–8 kDa-cutoff membrane SpectraPor®® Standard Grade RC Membrane) first against tap water (for 48 h) and then distilled water (for 20 h), lyophilized, and weighed. Carbohydrate content was evaluated by phenol–sulfuric acid method using glucose as the standard [40].

To characterize the EPS, ^{1}H NMR and ^{13}C NMR spectra of the EPS (5 mg mL^{-1} D_2O) were recorded with a Varian 500 MHz spectrophotometer at room temperature (25 °C). Spectra were recorded in D_2O and acetone-d_6 was used as the internal standard.

2.3. Evaluation of As^{III} or As^{V} Absorbed to EPS by Mass Spectroscopy

2.3.1. Standard and Reagents

All solutions were prepared with ultrapure water (resistivity 18.2 MΩcm) obtained with a Milli-Q water purification system (Semplicity, Newton, MA, USA, Millipore Milli-Q, Burlington, MA, USA). All glassware was washed with a 10% (*v*/*v*) HNO_3 solution and rinsed three times with Milli-Q water. Palladium powder and $Mg(NO_3)_2$ were supplied by Merck (Merck, Milan, Italy). Standard stock solution (100 ppm) of As was provided by Agilent Technologies, Inc. (Santa Clara, CA, USA). All reagents used were of analytical grade (Merck KGaA, Darmstadt, Germany).

2.3.2. Graphite Furnace Atomic Absorption Spectrometry (GF-AAS)

The determination of arsenic in aqueous samples was carried out according to the EPA method 200.9, Revision 2.2, available in electronic format from the following website: http://www.nemi.gov (accessed on 3 January 2023). This method reports the procedure for the determination of 16 elements, which includes arsenic, by GF-AAS. In the present study, the As analysis was carried out using a spectrophotometer (AA Varian model 220/Zeeman) and graphite furnace autosampler (Varian Australia, Mulgrade, VIC, Australia), equipped with a single-element hollow cathode lamp and a matrix modifier containing 0.015 mg Pd and 0.01 mg $Mg(NO_3)_2$. The calibration standards and the instrument performance were acceptable (Table 2). Good laboratory practice was applied throughout and procedural blanks were also analyzed.

Table 2. Performance data of the analytical method.

Performance Data	Results
Method detection limit (MDL) (µg L^{-1})	0.5
Instrumental detection limit (IDL) (µg/L)	1.5
Linearity (R^2)	0.9991
Calibration range (µg L^{-1})	20–100
Recovery (%)	95

2.3.3. Setup Absorption Experiments

The As absorption by the EPS was evaluated according to Naveed et al. [41] with some modifications. Briefly, the lyophilized EPS was dissolved in 2 mL of ultrapure water to obtain two solutions with different final concentrations of 100 and 300 µg mL^{-1}. Afterward, the EPS solutions were spiked with 2000 µg mL^{-1} solution in ultrapure water of $NaAsO_2$ (As^{III}) or Na_2HAsO_4 $7H_2O$ (As^{V}), with pH values of 7.8 and 7.4, respectively, and incubated at 30 °C for 30 min in a rotary shaker (150 rpm) to allow for the biosorption process. As^{III} or As^{V} solutions (without EPS were used as the control. Then, all the solutions were dialyzed through a 6–8 kDa-cutoff membrane (SpectraPor®® Standard Grade RC Membrane) for

12 h. The As remaining inside the tube after dialysis (As bonded to EPS) was measured using atomic absorption spectrometry, and the percentage of As adsorbed to EPS was determined by the following formula:

$$As\ adsorbed(\%) = \frac{As_e}{As_i} \times 100$$

where As_e and As_i represent the As final concentration with EPS and without EPS after dialysis, respectively.

2.4. Evaluation of Changes in the Chemical Structure of the EPS in the Presence of As^{III} or As^{V} by ATR-FTIR

Aliquots (100 µL) of the EPS dissolved in ultrapure water (EPS final concentration 300 µg mL^{-1}) were added in tubes (900 µL) containing the stock solutions of As^{III} or As^{V}, prepared as above, and finally dehydrated by evaporation.

An ATR-FTIR Vertex 70 V spectrometer (Bruker Optics), using Platinum diamond ATR, was employed to collect the spectra of As^{III}, As^{V}, EPS, and EPS after treatment with the two arsenic forms. All the spectra were obtained by collecting 48 scans with a resolution of 4 cm^{-1} in the 4000 to 400 cm^{-1} wavenumber range. The following data procedures were applied: (i) a baseline correction, in order to diminish the dissimilarities between spectra due to baseline shift; (ii) a smoothing treatment to reduce the instrumental noise; (iii) a first derivative treatment to correct the baseline shift together, and a second derivative treatment to better discriminate features associated with spectra; and (iv) a spectral normalization to correct the path-length variation and reduce the differences among the single measurements [42].

2.5. Toxicity Tests by Bioluminescent Assay

Vibrio harveyi strain G5 [43] was inoculated in the standard medium Sea Water Complete (composed by tryptone 5 g L^{-1}, yeast extract 3 g L^{-1}, glycerol 3 mL L^{-1}, 250 mL L^{-1} of seawater, and 750 mL L^{-1} of distilled water) and incubated at 28 °C. Aliquots (80 µL) of overnight culture of *V. harveyi* (OD_{600nm} = 0.5, equivalent to 5 × 10^8 bacteria mL^{-1}) were poured in a 96-well microtiter plate and 10 µL solution of each As form, dissolved in 2% NaCl (final concentration ranging from 500 to 4000 µg mL^{-1}), and 10 µL of each EPS stock solution (100 or 300 µg mL^{-1}) was added to each well. Wells without arsenic were used as the control.

Luminescence of the cell suspension was evaluated after 15 min of incubation at 25 °C and expressed as arbitrary units (a.u.). The toxicity was calculated by EC_{50}, as the effective concentration at which a 50% reduction in the light emission occurred, relative to the control.

2.6. Statistical Analysis

The experiments were carried out in triplicate and the data were expressed as the averages and standard deviations or relative errors (where specified). To compare the different experimental groups, data were analyzed by two-way ANOVA, and the Tukey's test was used for post hoc analysis (GraphPad Software Inc., La Jolla, CA, USA). All statistical values were considered significant at $p \leq 0.05$ or highly significant at $p \leq 0.01$.

3. Results

3.1. B. licheniformis B3-15 Resistance to $As^{(III)}$ or $As^{(V)}$

The ability to grow of *B. licheniformis* B3-15 in $MB\frac{1}{4}$ in the presence of As^{III} or As^{V} at different concentrations (500, 1000, 1500, 2000 µg mL^{-1}) is reported in Table 3.

B. licheniformis B3-15 showed "low growth" in the presence of As^{III} at 500 µg mL^{-1} after incubation at 45 °C for 48 and 72 h. In contrast, in the presence of As^{V} at 500 µg mL^{-1}, its growth was "low" after 24 h, increased to "medium" after 48 h, and "high" after 72 h of

incubation. The bacterial growth was "low" in the presence of As^V (1000 and 1500 μg mL^{-1}) after 48 h and 72 h. Finally, it was "low" at 2000 μg mL^{-1} after 72 h of incubation.

Table 3. *B. licheniformis* B3-15 growth in MB$\frac{1}{4}$ plus As^{III} or As^V at different concentrations. Absorbance values (OD_{600nm}) ≤ 0.2 were indicative for "no growth" (−), those ranging from 0.2 to 0.5 for "low growth" (+), from 0.5 to 0.8 for "medium growth" (++), and ≥0.8 for "high growth" (+++).

As^{III} (μg mL^{-1})					As^V (μg mL^{-1})				
Time (h)	**500**	**1000**	**1500**	**2000**	**Time (h)**	**500**	**1000**	**1500**	**2000**
24	−	−	−	−	24	+	−	−	−
48	+	−	−	−	48	++	+	+	−
72	+	−	−	−	72	+++	+	+	+

3.2. EPS B3-15 Production and Characterization

Under the optimal conditions of growth (temperature 45 °C, pH 8 and NaCl 2%) in the medium SG17, the strain B3-15 reached the highest growth ($OD_{600\,nm}$ = 1.19 ± 0.03) after 48 h of incubation and the EPS B3-15 yield was 240 mg L^{-1}.

The ^{1}H-NMR spectrum of EPS B3-15 registered in D_2O (Figure 1a) showed two anomeric signals at 5.28 and 5.06 ppm, suggesting a disaccharide repeating unit as the main component, with monomers connected by α-1,4 glycosidic linkages, having a little coupling constant, likely due to a manno-configuration. This observation was confirmed by the ^{13}C-NMR spectrum (Figure 1b), as an evident signal was detected in the anomeric carbon region at 104.15 ppm, attributed to C1, which was high field shifted due to the coupling between the anomer carbon in the (1–4)-linked mannose. Furthermore, the signal at 59.91 ppm in the ^{13}C-NMR spectrum could be attributed to C6, and the remaining signals (80.26, 76.29, 75.20, 63.32 ppm) were typical of the carbohydrate units and confirmed the presence of a pyranosidic hexose (i.e., mannose).

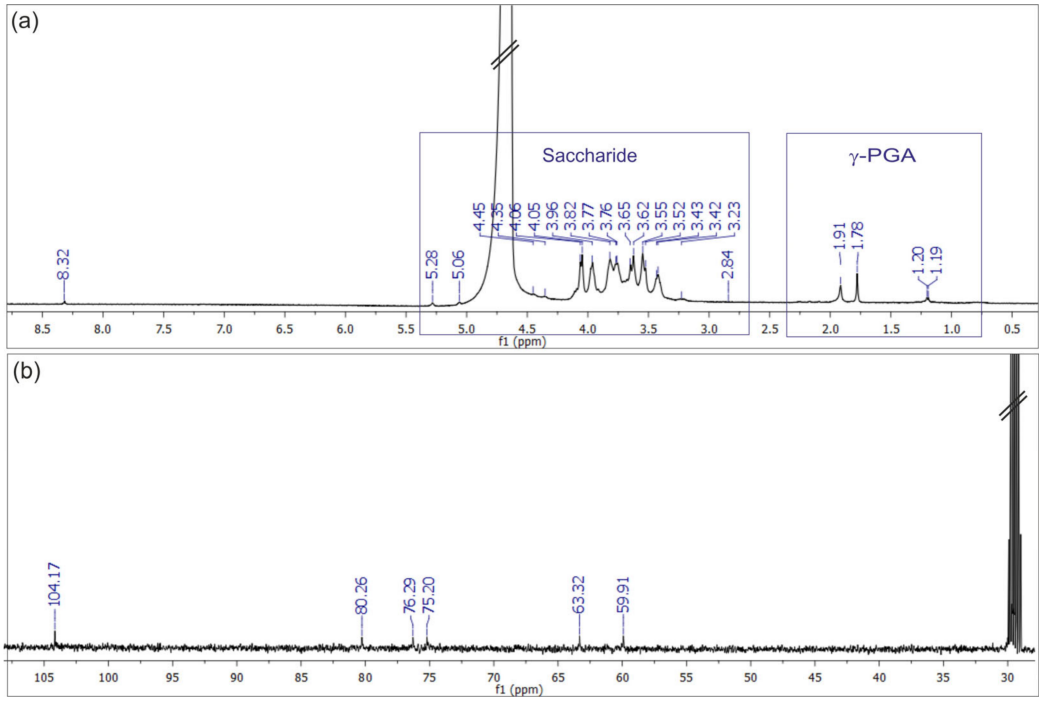

Figure 1. (**a**) ^{1}H-NMR and (**b**) ^{13}C-NMR spectra of crude EPS B3-15.

Moreover, the ^{1}H NMR spectral region between 1 and 2 ppm (Figure 1a) contained signals at 1.92 and 1.78 ppm, ascribable to the β-CH_2 and γ-CH protons of the poly-glutamic acid (γ-PGA) polymers, respectively. The signal related to the α-CH proton of

γ-PGA polymers was buried underneath the main proton peaks of the exopolysaccharide. Interestingly, when the spectrum was recorded with a 0.1% of acetone-d6 as the internal standard, the original single peak at 1.92 ppm split into two singlets (1.92 and 1.93 ppm) related to the two β-CH_2 protons, further confirming the presence of γ-PGA into the EPS B3-15 sample. Based on the NMR analyses, the crude EPS B3-15 was composed mainly of carbohydrates, with mannose and glucose as the major monosaccharides, and also by a minor component of γ-PGA.

3.3. Evaluation of As^{III} or As^{V} Absorbed to the EPS by Mass Spectroscopy

The ability of the EPS B3-15 (100 and 300 μg mL^{-1}) to adsorb As^{III} or As^{V} is reported in Figure 2.

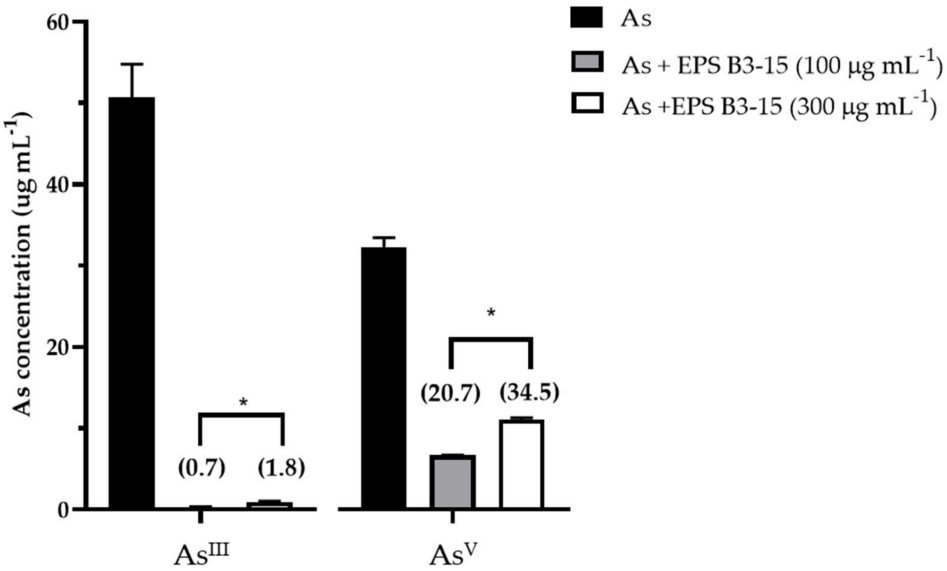

Figure 2. As^{III} and As^{V} concentration before and after 30 min treatment with EPS B3-15 (100 or 300 μg mL^{-1}). In brackets are the data of EPS adsorption expressed in percentage. * Significantly different ($p \leq 0.01$).

After 30 min of treatment, the As adsorption significantly increased ($p \leq 0.01$) with the addition of EPS B3-15 (100 and 300 μg mL^{-1}), with As^{V} (6.7 and 11.1 μg mL^{-1}, respectively) absorbed more efficiently than As^{III} (0.3 and 0.9 μg mL^{-1}, respectively).

3.4. Evaluation of Changes in the Chemical Structure of EPS B3-15 in the Presence of As^{III} or As^{V} by ATR-FTIR

The attenuated total reflectance Fourier transform infrared (ATR-FTIR) spectroscopic technique was applied to determine the molecular and conformational changes of EPS B3-15 after exposition to As^{III} or As^{V} at 2000 μg L^{-1}. The ATR-FTIR wavenumber values and their assignment to the different functional groups of the EPS and arsenic forms are reported in Table 4. The ATR-FTIR spectra of the EPS B3-15 in the presence of As^{III} or As^{V} are reported in Figure 3.

Table 4. ATR-FIR wavenumber values and assignment to functional groups of EPS, As^{III}, and As^{V}.

Wavenumber Values (cm^{-1})	Assignment	References
4000–2500	OH, stretching	[44]
3300–3200	Amide A	[45,46]
3000–2800	CH_2 and CH_3 of lipids	[47]
1710–1590	C=O	[48]
1550–1500	N-O stretching	[49]
~1548	Amide II peptide conformation	[46]
1456–1453	-CH_2 of lipids	[46]
1300–1200	C-O stretching	[48]
~1250	CH-NH stretching	[50]
~1066	(R-O-*p*-O-R) from ring vibration of carbohydrates	[51]
1060–1000	C-O	[48]
890–870	OH bending, stretching of the glycosidic bond	[48]
840–820	$AsO_3(OH)$	This study
878–792	AsO_4	This study
840–790	C=C bending	[48]
580–530	C-C-N	[48]
546–534	As	This study
480–430	C-C	[48]

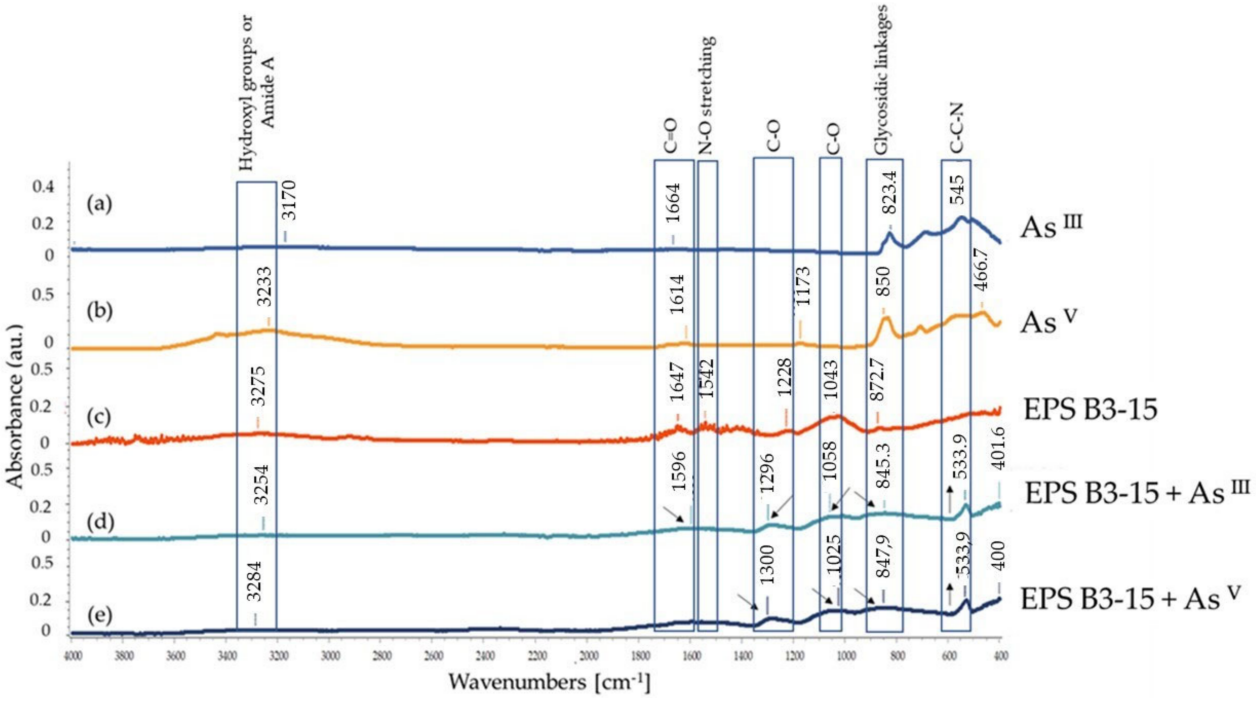

Figure 3. Comparison of the ATR-FTIR spectra of: (**a**) As^{III}, (**b**) As^{V}, (**c**) EPS B3-15 (300 μg mL^{-1}), (**d**) in the presence of arsenic As^{III}, or (**e**) As^{V} (2000 μg mL^{-1}). The main changes in the spectra are indicated as new (up arrows) or shifted peaks (left or right arrows).

In all of the spectra, the contribution of stretching in the frequency region 3500–3200 cm^{-1} could be related to the vibrations of hydroxyl groups or amide A [33,42]. In the EPS spectrum, the C=O stretching vibration peak (1647 cm^{-1}) and that of N–O stretching (1542 cm^{-1}) can be attributed to sugar units and polyglutamic acid (γ-PGA), respectively [48] (Figure 3c). Moreover, the EPS spectrum showed characteristic peaks that are peculiar of exopolysaccharides (1200–950 cm^{-1}) as well as spectral components that may be associated with α-(1→4) glycosidic linkages (970–920 cm^{-1}) [51] (Figure 3c).

The spectra of EPS in the presence of As^{III} or As^{V} showed several changes, and more specifically, the occurrence of new peaks or peak shifts (as indicated by the arrows in Figure 3d,e) were observed. The peak attributed to glycosidic bonds of EPS (872.7 cm^{-1}) (Figure 3c) moved to 845.3 cm^{-1} in the presence of As^{III} (Figure 3d) and to 847.9 cm^{-1} in

the presence of As^V (Figure 3e), often attributed to the formation of new bonds between the EPS and As^{III} or As^V. After As^{III} treatment, the amide II peak (1542 cm^{-1}) disappeared and was replaced by a new peak at 1596 cm^{-1}, indicating that the γ-PGA component may play a role in As^{III} adsorption (Figure 3d). In contrast, in the presence of As^V, no peaks were detected in the band, suggesting a different intramolecular arrangement of the same EPS (Figure 3e). In the EPS spectrum, the peak centered at 1228 cm^{-1} (Figure 3c) shifted to 1296 cm^{-1} in the presence of As^{III} (Figure 3d) and to 1300 cm^{-1} in the presence of As^V (Figure 3e), indicating a stronger interaction between the EPS and As^V rather than As^{III}. Interestingly, the peak corresponding to the stretching of the C–O bond (1043 cm^{-1}) shifted at a higher frequency value in the presence of As^{III} (Figure 3d), whereas it shifted to 1025 cm^{-1} in the presence of As^V (Figure 3e). These results suggest the formation of new bonds between the EPS and As^V.

3.5. Bioluminescent Assay

The effects of different concentrations (from 0 to 4000 μg mL^{-1}) of As^{III} or As^V on the luminescence of strain G5, in the absence or presence of the EPS (100 or 300 μg mL^{-1}) are reported in Figure 4. The luminescence intensity showed a sharp decrease when the concentration of As^{III} or As^V exceeded 2000 μg mL^{-1}.

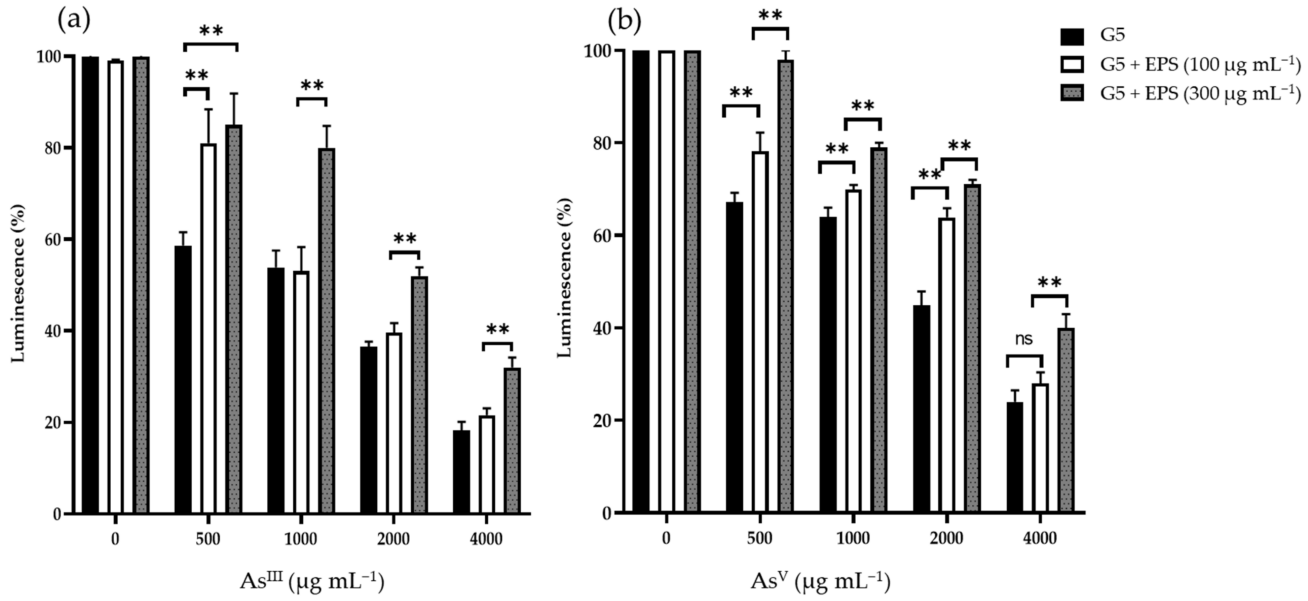

Figure 4. (**a**) As^{III} or (**b**) As^V toxicity expressed as a percentage of luminescence emitted by *V. harveyi* G5 (G5) after 15 min of incubation in the presence of EPS at two different concentrations (100 or 300 μg mL^{-1}). Not significantly different (ns) * Significantly different by ANOVA ($p \leq 0.05$) and ** ($p \leq 0.01$).

Effects on luminescence of strain G5 were determined for each arsenic form by the EC_{50} value (Figure 5). The EC_{50} values in the presence of As^{III} or As^V were 902 ± 26.8 μg mL^{-1} (Figure 5a) and 1591.5 ± 13.9 μg mL^{-1} (Figure 5b), respectively. The addition of EPS of 300 μg mL^{-1} increased the EC_{50} values twofold of both arsenic forms (2159 μg mL^{-1} for As^{III}, and 3343 ± 28.9 μg mL^{-1} for As^V). These results suggest the protective role of the crude EPS B3-15 against the toxic effects of As.

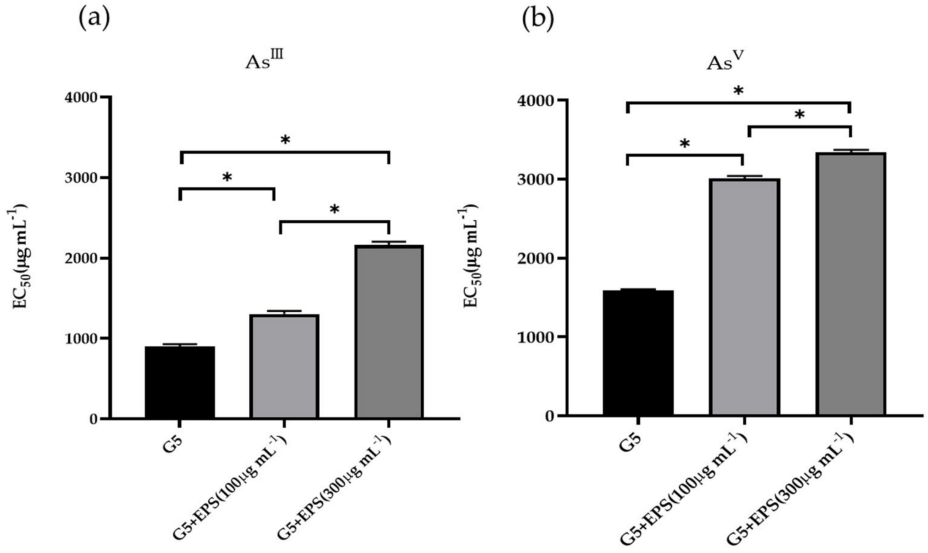

Figure 5. As^{III} (**a**) or As^{V} (**b**) toxicity expressed as EC_{50} on *V. harveyi* G5 (G5) after 15 min of incubation in the presence of EPS B3-15 (100 or 300 μg mL^{-1}). * Significantly different by ANOVA ($p \leq 0.01$).

4. Discussion

The elevated concentrations in the hydrothermal fluids of potentially toxic heavy metals including arsenic can lead to heavy metal resistance in the resident microbiota present at hydrothermal vents [20,22,52–54]. Exopolysaccharide (EPS) production represents an adaptive strategy developed by extremophiles to cope with environmental stresses. EPSs could play an important role in the removal of heavy metals from the environment as efficient flocculants as well as to adsorb metal ions from solutions [12,28]. In fact, for arsenic decontamination, different chemical and physical methods (such as adsorption, chemical precipitation, co-precipitation, electroplating, ion exchange, filtration, and reverse osmosis) are being extensively employed [55,56]. However, they have practical limitations (e.g., generation of toxic sludge, highly operational as well as maintenance costs) [57]. In this scenario, the biosorption of toxic heavy metals constitutes an attractive alternative to the commonly used physicochemical remediation processes.

Strain *B. licheniformis* B3-15, isolated from the shallow hydrothermal vent of Vulcano Is., was resistant to As^{III} at 500 μg mL^{-1}, whereas it was tolerant to As^{V} until 2000 μg mL^{-1}, which is generally less toxic than As^{III}. It is well-known that bacilli are able to produce a variety of exoproducts including lipopeptides and EPSs, depending on the culture conditions and the extraction procedures [28,33,58]. Moreover, it has been reported that the choice of nitrogen sources, as inorganic or organic nutrients, and carbon sources, highly influences the yield of EPSs [59,60]. In this study, the crude EPS B3-15 yield (240 mg L^{-1}) was 45% higher than previously reported [30] after 48 h of incubation in the novel SG17 medium. SG17 medium, containing a higher dose of glucose (5%) and different nitrogen sources (as meat and yeast extracts, 0.2%) than the previously used medium (i.e., MD162), increased both the growth and the EPS yield. However, the crude EPS production was not stimulated by higher carbon concentrations (until 10% *w*/*v*). When compared with other Eolian bacilli producing EPSs, the yield of the crude EPS by strain B3-15 was comparable with that produced by *B. licheniformis* strain T14 (256 mg L^{-1}, with sucrose) [32] and higher than that produced by strain 1A70 (185 mg L^{-1}, with ribose) and *B. horneckiae* SBP3 (70 mg mL^{-1}) isolated from Panarea Island [28]. Moreover, strain B3-15 produced higher amounts of EPS than those of *Geobacillus* spp. previously isolated from hot springs and marine vents such as *G. thermodenitrificans* strain B3-72 (70 mg L^{-1} with glucose) [61], *G. tepidamans* strain V264 (111.4 mg L^{-1}, with sucrose) [62], *Geobacillus* strain 4004 (65 mg L^{-1}, with sucrose), and *Geobacillus* strain 4001 (55 mg L^{-1}, with sucrose) [63].

The crude EPS B3-15 possessed a high carbohydrate content (67%), constituted by a disaccharide unit with a manno-pyranosidic configuration, as for the fraction EPS2 B3-

15 previously reported [30]. Moreover, it possessed low protein content (5%), mainly attributed to the poly-gamma glutamic acid component. This composition, assumed by NMR analysis, was confirmed by the ATR-FTIR spectrum of EPS B3-15, which showed signals attributed to the functional groups of the polysaccharide (4000–3000 cm^{-1}) and the γ-PGA (1550–1500 cm^{-1}) components. The comparison of the ATR-FTIR spectra of the EPS not treated and treated with As^{III} or As^{V} highlighted the role of the chemical groups of polysaccharide and γ-PGA in the As-binding process. The EPS B3-15 showed five prominent peaks after As^{III} treatment (Figure 3d). In particular, the appearance of the peak attributed to As^{III} and the disappearance of the peak attributed to the N–O group of γ-PGA suggests a link between γ-PGA and As^{III}. Conversely, the loss of the peaks attributed to N–O and C–O groups only in the EPS spectrum treated with As^{V} (Figure 3e) indicated a greater interaction between EPS and As^{V} than EPS and As^{III}.

Due to its chemical composition and structure, the EPS B3-15 at increasing concentrations (100 and 300 μg mL^{-1}) was able to adsorb As^{V} (11.1 μg mL^{-1}, equivalent to 36,000 μg per g of EPS) more efficiently than As^{III} (0.9 μg mL^{-1}, equivalent to 3000 μg per g of EPS).

To our knowledge, there is no work in the literature on the As adsorption by EPS from bacilli. Nonetheless, compared with the As^{III} absorbing ability of biomass from bacilli, EPS B3-15 was more efficient than the *B. pumilus* (5 μg g^{-1}) [64], *B. megaterium* (7 μg g^{-1}) [64], and *B. megaterium* strain UM-123 (127 μg g^{-1}) [65], whereas it was less active than *Bacillus* sp. DJ1 (9800 μg g^{-1}) [66], *B. thuringiensis* strain WS3 (10,940 μg g^{-1}) [67], and *Bacillus cereus* (32,240 μg g^{-1}) [68]. Moreover, EPS B3-15 absorbed As^{V} more efficiently than the biomass of *B. cereus* (30,040 μg g^{-1}) [69].

A bioluminescence inhibition assay, as a rapid (15 min) and reliable detecting tool, was used to determine the arsenic toxicity as well as the ability of the EPS to prevent toxic effects. One of the advantages of this test is that luminescence inhibition in microorganisms can efficiently display noxious effects on higher organisms in different environments [70]. This test confirmed that EPS B3-15, previously evaluated on human peripheral blood mononuclear cells, resulted in not being cytotoxic up to 300 μg mL^{-1} [34]. Moreover, in the presence of the EPS, the EC_{50} of As increased almost twofold, indicating a protective activity against the toxicity of both arsenic forms.

5. Conclusions

EPSs from thermophiles from shallow hydrothermal vents of the Eolian Islands are usually biodegradable, non-toxic, safe, and both environmental and human compatible [28,32], making these biopolymers promising candidates for industrial and pharmaceutical applications [33,36,38,58].

In this study, the yield of the EPS produced by *Bacillus licheniformis* B3-15 in the novel SG17 medium was higher (240 mg L^{-1}) than that previously reported. The crude EPS was constituted by a disaccharide repeating unit having a manno-pyranosidic configuration and low protein content, mainly attributed to the poly-γ-glutamic acid component. Due to its chemical composition, EPS B3-15 at the increasing concentration (100 and 300 μg mL^{-1}) was able to adsorb As^{V} (20.5% and 34.5%, respectively) more efficiently than As^{III} (0.7 and 1.8%, respectively) through glycosidic linkages and ion exchanges between the –OH groups and the formation of bonds with the γ-PGA component. In a bioluminescent assay, the presence of the EPS lowered the arsenic cytotoxicity more than twofold, suggesting a protective role against both arsenic forms.

The crude EPS B3-15 could be used without further chemical treatments in arsenic bioremediation as an eco-friendly alternative to physical or chemical methods.

Author Contributions: Conceptualization, A.S. (Antonio Spanò), V.Z. and C.G.; Data curation, D.T., S.M., M.M. and S.P.P.G.; Formal analysis, A.S. (Angela Scala) and C.G.; Investigation, A.S. (Antonio Spanò), V.Z., A.M., E.A., A.S. (Angela Scala), D.T., A.S. (Antonella Smeriglio), M.I. and M.T.C.; Methodology, A.M., Eleonora Agostino, A.S. (Angela Scala), D.T., A.S. (Antonella Smeriglio) and M.T.C.; Software, E.A. and M.T.C.; Supervision, S.M., S.P.P.G. and C.G.; Validation, M.S.N., S.M. and C.G.L.; Visualization, V.Z.; Writing—original draft, A.S. (Antonio Spanò), V.Z. and A.S. (Antonella

Smeriglio); Writing—review & editing, M.S.N., M.M., C.G.L. and C.G. All authors have read and agreed to the published version of the manuscript.

Funding: A.M., E.A., M.S.N. and V.Z. were supported by "PON "Ricerca e Innovazione" 2014–2020". This research was supported by PON2 2013-2015 "Marine Hazard" PON03PE_00203.

Institutional Review Board Statement: Not applicable.

Informed Consent Statement: Not applicable.

Data Availability Statement: Not applicable.

Conflicts of Interest: The authors declare no conflict of interest.

Abbreviations

As: arsenic; ATR-FTIR: attenuated total reflectance Fourier transform infrared; CFS: cell-free supernatant; EPSs: exopolysaccharides.

References

1. Shaji, E.; Santosh, M.; Sarath, K.V.; Prakash, P.; Deepchand, V.; Divya, B.V. Arsenic contamination of groundwater: A global synopsis with focus on the Indian Peninsula. *Geosci. Front.* **2021**, *12*, 101079. [CrossRef]
2. Smedley, P.L.; Kinniburgh, D.G. Arsenic in groundwater and the environment. In *Essentials of Medical Geology*; Selinus, O., Ed.; Springer: Dordrecht, The Netherlands, 2013; pp. 279–310.
3. Sharma, V.K.; Sohn, M. Aquatic arsenic: Toxicity, speciation, transformations, and remediation. *Environ. Int.* **2009**, *35*, 743–759. [CrossRef]
4. Casentini, B.; Gallo, M.; Baldi, F. Arsenate and arsenite removal from contaminated water by iron oxides nanoparticles formed inside a bacterial exopolysaccharide. *J. Environ. Chem. Eng.* **2019**, *7*, 102908. [CrossRef]
5. Leon, C.G.; Moraga, R.; Valenzuela, C.; Gugliandolo, C.; Lo Giudice, A.; Papale, M.; Vilo, C.; Dong, Q.; Smith, C.T.; Rossello-mora, R.; et al. Effect of the natural arsenic gradient on the diversity and arsenic resistance of bacterial communities of the sediments of Camarones River (Atacama Desert, Chile). *PLoS ONE* **2018**, *13*, e0195080. [CrossRef]
6. Singh, R.; Singh, S.; Parihar, P.; Singh, V.P.; Prasad, S.M. Arsenic contamination, consequences and remediation techniques: A review. *Ecotoxicol. Environ. Saf.* **2015**, *112*, 247–270.
7. Gupta, P.; Diwan, B. Bacterial Exopolysaccharide mediated heavy metal removal: A review on biosynthesis, mechanism and remediation strategies. *Biotechnol. Rep.* **2017**, *13*, 58–71. [CrossRef]
8. Pintor, A.M.A.; Ferreira, C.I.A.; Pereira, J.C.; Correia, P.; Silva, S.P.; Vilar, V.J.P.; Botelho, C.M.S.; Boaventura, R.A.R. Use of cork powder and granules for the adsorption of pollutants: A review. *Water Res.* **2012**, *46*, 3152–3166. [CrossRef]
9. Alluri, H.K.; Ronda, S.R.; Settalluri, V.S.; Bondili, J.S.; Suryanarayana, V.; Venkateshwar, P. Biosorption: An eco-friendly alternative for heavy metal removal. *Afr. J. Biotechnol.* **2007**, *6*, 2924–2931.
10. Wei, Y.; Zhao, Y.; Zhao, X.; Gao, X.; Zheng, Y.; Zuo, H.; Wei, Z. Roles of different humin and heavy-metal resistant bacteria from composting on heavy metal removal. *Bioresour. Technol.* **2020**, *296*, 122375. [CrossRef]
11. Decho, A.W.; Gutierrez, T. Microbial extracellular polymeric substances (EPSs) in ocean systems. *Front. Microbiol.* **2017**, *8*, 92. [CrossRef]
12. Nicolaus, B.; Kambourova, M.; Oner, E.T. Exopolysaccharides from extremophiles: From fundamentals to biotechnology. *Environ. Technol.* **2010**, *31*, 1145–1158. [CrossRef]
13. Finore, I.; Di Donato, P.; Mastascusa, V.; Nicolaus, B.; Poli, A. Fermentation technologies for the optimization of marine microbial exopolysaccharide production. *Mar. Drugs* **2014**, *12*, 3005–3024. [CrossRef]
14. Poli, A.; Anzelmo, G.; Nicolaus, B. Bacterial exopolysaccharides from extreme habitat: Production, characterization and biological activities. *Mar. Drugs* **2010**, *8*, 1779–1802. [CrossRef]
15. Mota, R.; Rossi, F.; Andrenelli, L.; Pereira, S.B.; De Philippis, R.; Tamagnini, P. Released polysaccharides (RPS) from *Cyanothece* sp. CCY 0110 as biosorbent for heavy metals bioremediation: Interactions between metals and RPS binding sites. *Appl. Microbiol. Biotechnol.* **2016**, *100*, 7765–7775. [CrossRef]
16. Zhu, X.L.; Lv, B.X.; Shang, X.Q.; Wang, J.Q.; Li, M.; Yu, X.Y. The immobilization effects on Pb, Cd and Cu by the inoculation of organic phosphorus-degrading bacteria (OPDB) with rapeseed dregs in acidic soil. *Geoderma* **2019**, *350*, 1–10. [CrossRef]
17. Dando, P.R.; Stuben, D.; Varnavas, S.P. Hydrothermalism in the Mediterranean Sea. *Prog. Oceanogr.* **1999**, *44*, 333–367. [CrossRef]
18. Karuza, A.; Celussi, M.; Cibic, T.; Del Negro, P.; De Vittor, C. Virioplankton and bacterioplankton in a shallow CO_2-dominated hydrothermal vent (Panarea Island, Tyrrhenian Sea). *Estuar. Coast. Shelf Sci.* **2012**, *97*, 10–18. [CrossRef]
19. Price, R.E.; Savov, I.; Planer-Friedrich, B.; Bühring, S.; Amend, J.; Pichler, T. Processes influencing extreme As enrichment in shallow-sea hydrothermal fluids of Milos Island, Greece. *Chem. Geol.* **2013**, *348*, 15–26. [CrossRef]
20. Price, R.E.; London, J.; Wallschläger, D.; Ruiz-Chancho, M.J.; Pichler, T. Enhanced bioaccumulation and biotransformation of As in coral reef organisms surrounding a marine shallow-water hydrothermal vent system. *Chem. Geol.* **2013**, *348*, 48–55. [CrossRef]

21. Price, R.E.; Lesniewski, R.; Nitzsche, K.; Meyerdierks, A.; Saltikov, C.; Pichler, T.; Amend, J. Archaeal and bacterial diversity in an arsenic-rich shallow-sea hydrothermal system undergoing phase separation. *Front. Microbiol.* **2013**, *4*, 158. [CrossRef]
22. Price, R.E.; Larowe, D.E.; Italiano, F.; Savov, I.; Pichler, T.; Amend, J.P. Subsurface hydrothermal processes and the bioenergetics of chemolithoautotrophy at the shallow-sea vents off Panarea Island (Italy). *Chem. Geol.* **2015**, *408*, 21–45. [CrossRef]
23. Rusch, A.; Amend, J.P. Functional characterization of the microbial community in geothermally heated marine sediments. *Microb. Ecol.* **2008**, *55*, 723–736. [CrossRef]
24. Varnavas, S.P.; Cronan, D.S. Arsenic, antimony and bismuth in sediments and waters from the Santorini hydrothermal field, Greece. *Chem. Geol.* **1988**, *67*, 295–305. [CrossRef]
25. Zammuto, V.; Fuchs, F.M.; Fiebrandt, M.; Stapelmann, K.; Ulrich, N.J.; Maugeri, T.L.; Pukall, R.; Gugliandolo, C.; Moeller, R. Comparing spore resistance of *Bacillus* strains isolated from hydrothermal vents and spacecraft assembly facilities to environmental stressors and decontamination treatments. *Astrobiology* **2018**, *18*, 1425–1434. [CrossRef]
26. Zammuto, V.; Rizzo, M.G.; De Plano, L.M.; Franco, D.; Guglielmino, S.; Caccamo, M.T.; Magazù, S.; Fujimori, A.; Lo Giudice, A.; Guglielmin, M.; et al. Effects of heavy ion particle irradiation on spore germination of *Bacillus* spp. from extremely hot and cold environments. *Life* **2020**, *10*, 264. [CrossRef]
27. Zammuto, V.; Caccamo, M.T.; Magazù, S.; Spanò, A.; Guglielmino, S.; Gugliandolo, C. Hot resistance of spores from the thermophilic *Bacillus horneckiae* SBP3 of shallow hydrothermal vent origin elucidated by spectroscopic analyses. *Appl. Sci.* **2021**, *11*, 4256. [CrossRef]
28. Gugliandolo, C.; Lentini, V.; Spanò, A.; Maugeri, T.L. New bacilli from shallow hydrothermal vents of Panarea Island (Italy) and their biotechnological potentialities. *J. Appl. Microbiol.* **2012**, *112*, 1102–1112. [CrossRef]
29. Maugeri, T.L.; Gugliandolo, C.; Caccamo, D.; Stackebrandt, E. Three novel halotolerant and thermophilic *Geobacillus* strains from shallow marine vents. *Syst. Appl. Microbiol.* **2002**, *25*, 450–455. [CrossRef]
30. Maugeri, T.L.; Gugliandolo, C.; Caccamo, D.; Panico, A.; Lama, L.; Gambacorta, A.; Nicolaus, B. A halophilic thermotolerant *Bacillus* isolated from a marine hot spring able to produce a new exopolysaccharide. *Biotechnol. Lett.* **2002**, *24*, 515–519. [CrossRef]
31. Lentini, V.; Gugliandolo, C.; Maugeri, T.L. Identification of enzyme-producing thermophilic bacilli isolated from marine vents of Aeolian Islands (Italy). *Ann. Microbiol.* **2007**, *57*, 355–361. [CrossRef]
32. Spano, A.; Gugliandolo, C.; Lentini, V.; Maugeri, T.L.; Anzelmo, G.; Poli, A.; Nicolaus, B. A novel EPS-producing strain of *Bacillus licheniformis* isolated from a shallow vent off Panarea Island (Italy). *Curr. Microbiol.* **2013**, *67*, 21–29. [CrossRef]
33. Zammuto, V.; Spanò, A.; Nicolò, M.S.; Grillo, E.; Caccamo, M.T.; Magazù, S.; Cappello, S.; Gugliandolo, C. Thermophilic hydrocarbon-utilizing bacilli from marine shallow hydrothermal vents as producers of biosurfactants. *J. Mar. Sci. Eng.* **2022**, *10*, 1077. [CrossRef]
34. Arena, A.; Maugeri, T.L.; Pavone, B.; Jannello, D.; Gugliandolo, C.; Bisignano, G. Antiviral and immunoregulatory effect of a novel exopolysaccharide from a marine thermotolerant *Bacillus licheniformis*. *Int. Immunopharmacol.* **2006**, *6*, 8–13. [CrossRef]
35. Arena, A.; Gugliandolo, C.; Stassi, G.; Pavone, B.; Iannello, D.; Bisignano, G.; Maugeri, T.L. An exopolysaccharide produced by *Geobacillus thermodenitrificans* strain B3-72: Antiviral activity on immunocompetent cells. *Immunol. Lett.* **2009**, *123*, 132–137. [CrossRef]
36. Gugliandolo, C.; Spanò, A.; Lentini, V.; Arena, A.; Maugeri, T.L. Antiviral and immunomodulatory effects of a novel bacterial exopolysaccharide of shallow marine vent origin. *J. Appl. Microbiol.* **2014**, *116*, 1028–1034. [CrossRef]
37. Gugliandolo, C.; Spano, A.; Maugeri, T.L.; Poli, A.; Arena, A.; Nicolaus, B. Role of bacterial exopolysaccharides as agents in counteracting immune disorders induced by herpes virus. *Microorganisms* **2015**, *3*, 464–483. [CrossRef]
38. Spanò, A.; Laganà, P.; Visalli, G.; Maugeri, T.L.; Gugliandolo, C. In vitro antibiofilm activity of an exopolysaccharide from the marine thermophilic *Bacillus licheniformis* T14. *Curr. Microbiol.* **2016**, *72*, 518–528. [CrossRef]
39. Spanò, A.; Arena, A. Bacterial exopolysaccharide of shallow marine vent origin as agent in counteracting immune disorders induced by Herpes virus. *J. Immunoas. Immunoch.* **2016**, *37*, 251–260. [CrossRef]
40. Dubois, M.; Gilles, K.A.; Hamilton, J.K.; Rebers, P.A.; Smith, F. Colorimetric Method for Determination of Sugars and Related Substances. *Anal. Chem.* **1956**, *28*, 350–356. [CrossRef]
41. Naveed, S.; Li, C.; Zhang, J.; Zhang, C.; Ge, Y. Sorption and transformation of arsenic by extracellular polymeric substances extracted from *Synechocystis* sp. PCC6803. *Ecotoxicol. Environ. Saf.* **2020**, *206*, 111200. [CrossRef]
42. Caccamo, M.T.; Gugliandolo, C.; Zammuto, V.; Magazù, S. Thermal properties of an exopolysaccharide produced by a marine thermotolerant *Bacillus licheniformis* by ATR-FTIR spectroscopy. *Int. J. Biol. Macromol.* **2020**, *145*, 77–83. [CrossRef]
43. Zammuto, V.; Rizzo, M.G.; Spanò, A.; Genovese, G.; Morabito, M.; Spagnuolo, D.; Capparucci, F.; Gervasi, C.; Smeriglio, A.; Trombetta, D.; et al. In vitro evaluation of antibiofilm activity of crude extracts from macroalgae against pathogens relevant in aquaculture. *Aquaculture* **2022**, *549*, 737729. [CrossRef]
44. Wang, Y.-X.; Xin, Y.; Yin, J.-Y.; Huang, X.-J.; Wang, J.-Q.; Hu, J.-L.; Geng, F.; Nie, S.-P. Revealing the architecture and solution properties of polysaccharide fractions from *Macrolepiota albuminosa* (Berk.) *Pegler*. *Food Chem.* **2022**, *368*, 130772. [CrossRef]
45. Arrondo, J.L.; Goñi, F.M. Special Issue: Infrared spectroscopy of membrane lipids. *Chem. Phys. Lipids* **1998**, *96*, 1–164.
46. Naumann, D.; Fabian, H.; Lasch, P. FTIR spectroscopy of cells, tissues and body fluids. In *Advances in Biomedical Spectroscopy*; IOSPress BV: Amsterdam, The Netherlands, 2009; Volume 2, pp. 312–354.

47. Yoshida, S.; Miyazaki, M.; Sakai, K.; Takeshita, M.; Yuasa, S.; Sato, A.; Kobayashi, T.; Watanabe, S.; Okuyama, H. Fourier Transform Infrared spectroscopic analysis of rat brain microsomal membranes modified by dietary fatty acids: Possible correlation with altered learning behavior. *Biospectroscopy* **1997**, *3*, 281–290. [CrossRef]
48. El Farissi, H.; Talhaoui, A.; EL Bachiri, A. Influence of pyrolysis process on the production of bio-oil used as alternative green energy from *Pistacia lentiscus* L. *J. Anal. Appl. Pyrolys.* **2022**, *168*, 105781. [CrossRef]
49. Wiercigroch, E.; Szafraniec, E.; Czamara, K.; Pacia, M.Z.; Majzner, K.; Kochan, K.; Kaczor, A.; Baranska, M.; Malek, K. Raman and infrared spectroscopy of carbohydrates: A review. *Spectrochim. Acta Part A Mol. Biomol. Spectr.* **2017**, *185*, 317–335. [CrossRef]
50. Ramani, K.; Jain, S.C.; Mandal, A.B.; Sekaran, G. Microbial induced lipoprotein biosurfactant from slaughterhouse lipid waste and its application to the removal of metal ions from aqueous solution. *Colloids Surf. B.* **2012**, *97*, 254–263. [CrossRef]
51. Lee, Z.; Carder, K.; Arnone, R.; He, M. Determination of Primary Spectral Bands for Remote Sensing of Aquatic Environments. *Sensors* **2007**, *7*, 3428–3441. [CrossRef]
52. Breuer, C.; Pichler, T. Arsenic in marine hydrothermal fluids. *Chem. Geol.* **2013**, *348*, 2–14. [CrossRef]
53. Price, R.E.; Pichler, T. Distribution, speciation and bioavailability of arsenic in a shallow-water submarine hydrothermal system, Tutum Bay, Ambitle Island, PNG. *Chem. Geol.* **2005**, *224*, 122–135. [CrossRef]
54. Vetriani, C.; Chew, Y.S.; Miller, S.M.; Yagi, J.; Coombs, J.; Lutz, R.A.; Barkay, T. Mercury adaptation among bacteria from a deep-sea hydrothermal vent. *Appl. Environ. Microbiol.* **2005**, *71*, 220–226. [CrossRef]
55. Hassan, K.M.; Fukuhara, T.; Hai, F.I.; Bari, Q.H.; Islam, K.M.S. Development of a bio-physicochemical technique for arsenic removal from groundwater. *Desalination* **2009**, *249*, 224–229. [CrossRef]
56. Ungureanu, G.; Santos, S.; Boaventura, R.; Botelho, C. Arsenic and antimony in water and wastewater: Overview of removal techniques with special reference to latest advances in adsorption. *J. Environ. Manag.* **2015**, *151*, 326–342. [CrossRef]
57. Srivastava, S.; Anil Dwivedi, K. Biological wastes the tool for biosorption of arsenic. *J. Bioremed. Biodegrad.* **2015**, *7*, 2. [CrossRef]
58. Caccamo, M.T.; Zammuto, V.; Spanò, A.; Gugliandolo, C.; Magazù, S. Hydrating capabilities of the biopolymers produced by the marine thermophilic *Bacillus horneckiae* SBP3 as evaluated by ATR-FTIR spectroscopy. *Materials* **2022**, *15*, 5988. [CrossRef]
59. Larpin, S.; Sauvageot, N.; Pichereau, V.; Laplace, J.M.; Auffray, Y. Biosynthesis of exopolysaccharide by a *Bacillus licheniformis* strain isolated from ropy cider. *Int. J. Food Microbiol.* **2002**, *77*, 1–9. [CrossRef]
60. Asgher, M.; Qamar, S.A.; Bilal, M.; Iqbal, H.M.N. Bio-based active food packaging materials: Sustainable alternative to conventional petrochemical-based packaging materials. *Food Res. Int.* **2020**, *137*, 109625. [CrossRef]
61. Nicolaus, B.; Panico, A.; Manca, M.C.; Lama, L.; Gambacorta, A.; Maugeri, T.L. A thermophilic *Bacillus* isolated from an Eolian shallow hydrothermal vent, able to produce exopolysaccharides. *Syst. Appl. Microbiol.* **2000**, *23*, 426–432. [CrossRef]
62. Kambourova, M.; Mandeva, R.; Dimova, D.; Poli, A.; Nicolaus, B.; Tommonaro, G. Production and characterization of a microbial glucan, synthesized by *Geobacillus tepidamans* V264 isolated from Bulgarian hot spring. *Carbohydr. Polym.* **2009**, *77*, 338–343. [CrossRef]
63. Nicolaus, B.; Lama, L.; Panico, A.; Schiano Moriello, V.; Romano, I.; Gambacorta, A. Production and characterization of exopolysaccharides excreted by thermophilic bacteria from shallow, marine hydrothermal vents of Flegrean areas (Italy). *Syst. Appl. Microbiol.* **2002**, *25*, 319–325. [CrossRef] [PubMed]
64. Vishnoi, N.; Dixit, S.; Singh, D.P. Differential pattern of arsenic binding by the cell wall in two arsenite tolerant *Bacillus* strains isolated from arsenic contaminated soil. *Cell. Mol. Biol.* **2016**, *62*, 1000138.
65. Miyatke, M.; Hayashi, S. Characteristics of arsenic removal from aqueous solution by *Bacillus megaterium* strain UM-123. *J. Environ. Biotechnol.* **2009**, *9*, 123–129.
66. Joshi, D.N.; Flora, S.J.S.; Kalia, K. *Bacillus* sp. strain DJ-1, potent arsenic hypertolerant bacterium isolated from the industrial effluent of India. *J. Hazard. Mater.* **2009**, *66*, 1500–1505. [CrossRef]
67. Altowayti, W.A.H.; Algaifi, H.A.; Bakar, S.A.; Shahir, S. The adsorptive removal of As (III) using biomass of arsenic resistant *Bacillus thuringiensis* strain WS3: Characteristics and modelling studies. *Ecotoxicol. Environ. Saf.* **2019**, *172*, 176–185. [CrossRef]
68. Giri, A.K.; Patel, R.K.; Mahapatra, S.S.; Mishra, P.C. Biosorption of arsenic (III) from aqueous solution by living cells of *Bacillus cereus*. *Environ. Sci. Pollut. Res.* **2012**, *20*, 1281–1291. [CrossRef]
69. Giri, A.K.; Patel, R.K.; Mishra, P.C. Biosorption of As(V) from aqueous solutions by living cells of *Bacillus cereus*. *Water Sci. Technol.* **2012**, *66*, 1699–1707. [CrossRef]
70. Mohseni, M.; Abbaszadeh, J.; Maghool, S.S.; Chaichi, M.J. Heavy metals detection using biosensor cells of a novel marine luminescent bacterium *Vibrio* sp. MM1 isolated from the Caspian Sea. *Ecotoxicol. Environ. Saf.* **2018**, *148*, 555–560. [CrossRef]